

# SCIENTIFIC REPORTS



OPEN

## An Efficient Site-Specific Method for Irreversible Covalent Labeling of Proteins with a Fluorophore

Received: 20 April 2015  
Accepted: 07 September 2015  
Published: 19 November 2015

Jiaquan Liu<sup>1</sup>, Jeunghill Hanne<sup>1</sup>, Brooke M. Britton<sup>1</sup>, Matthew Shoffner<sup>1</sup>, Aaron E. Albers<sup>2</sup>, Jared Bennett<sup>1</sup>, Rachel Zatezalo<sup>1</sup>, Robyn Barfield<sup>2</sup>, David Rabuka<sup>2</sup>, Jong-Bong Lee<sup>3,4</sup> & Richard Fishel<sup>1,5</sup>

Fluorophore labeling of proteins while preserving native functions is essential for bulk Förster resonance energy transfer (FRET) interaction and single molecule imaging analysis. Here we describe a versatile, efficient, specific, irreversible, gentle and low-cost method for labeling proteins with fluorophores that appears substantially more robust than a similar but chemically distinct procedure. The method employs the controlled enzymatic conversion of a central Cys to a reactive formylglycine (fGly) aldehyde within a six amino acid Formylglycine Generating Enzyme (FGE) recognition sequence *in vitro*. The fluorophore is then irreversibly linked to the fGly residue using a Hydrazinyl-Iso-Pictet-Spengler (HIPS) ligation reaction. We demonstrate the robust large-scale fluorophore labeling and purification of *E. coli* (Ec) mismatch repair (MMR) components. Fluorophore labeling did not alter the native functions of these MMR proteins *in vitro* or *in singulo*. Because the FGE recognition sequence is easily portable, FGE-HIPS fluorophore-labeling may be easily extended to other proteins.

FRET and single molecule fluorescence tracking have become versatile tools in modern molecular biology<sup>1,2</sup>. Use of these techniques has greatly improved our understanding of many biophysical processes including replication<sup>3–7</sup>, transcription<sup>8–14</sup>, translation<sup>15–17</sup> and DNA repair<sup>18–22</sup>. These studies generally employ fluorescent molecules as an imaging tool<sup>3–5,8–11,15,16,19–21</sup>. A common fluorescence imaging technique employs quantum dot (QD) labeling. However, the size of the QDs (10–50 nm) can often exceed the size of the molecule that is being imaged. These issues may lead to unusual solution and diffusion characteristics of QD-labeled proteins. Moreover, detection of molecular interactions using FRET between appropriate QD excitation-emission pairs is inherently inefficient<sup>23</sup>. In contrast, numerous small chemical fluorophores display both high quantum yield and FRET efficiency.

Conventional methods employed for fluorophore-labeling of proteins often impact native function(s). This is especially true in the case of more chemically sensitive protein targets. A number of protein-fluorophore labeling methods have been reported including: Cys-maleimide chemistry, incorporation of non-natural reactive amino acids as well as peptide tags such as Halo(haloalkane dehalogenase), SNAP/CLIP(O<sup>6</sup>-alkylguanine-DNA alkyltransferase), Avi(biotin ligase recognition peptide), Sfp phosphopantetheinyl transferase(CoA), Sortase and others<sup>24</sup>. However, there are important limitations associated with these methods. For example, Cys-maleimide conjugation requires a single Cys residue located in a benign structural position of the protein target. Other methods suffer from low labeling efficiencies, require expensive reagents or result in abnormally large fluorophore-protein complexes<sup>24</sup>.

Recently, a site-specific conjugation method was described that relies on the incorporation of a six amino acid FGE recognition sequence, Leu-Cys-Thr-Pro-Ser-Arg (LCTPSR). Conversion of the central

<sup>1</sup>Department of Molecular Virology, Immunology and Medical Genetics, The Ohio State University Medical Center, Columbus, OH 43210. <sup>2</sup>Catalent Biologics–West, Emeryville, CA 94608. <sup>3</sup>Department of Physics, Pohang University of Science and Technology (POSTECH), Pohang, Korea. <sup>4</sup>School of Interdisciplinary Bioscience and Bioengineering, POSTECH, Pohang, Korea. <sup>5</sup>Physics Department, The Ohio State University, Columbus, OH 43210. Correspondence and requests for materials should be addressed to R.F. (email: rfishel@osu.edu)

Cys residue to an fGly produces a reactive aldehyde that may then be used for chemical coupling<sup>25–27</sup>. Co-expression of FGE with LCTPSR-containing target proteins appeared to catalyze Cys → fGly conversion *in vivo* permitting chemical coupling of a hydrazide-modified fluorophore<sup>1</sup>. Although substantial fluorophore labeling was reported a number of technical issues arose that included: (1) the use of large quantities of expensive hydrazide-modified dyes (75.6 mM; 60 mg Cy3/ml) to obtain extensive labeling, (2) the conversion of Cys to fGly *in vivo* was not quantified, (3) the specificity of fluorophore labeling to the fGly residue was not determined, and (4) the effects of the labeling process on overall protein specific-activity was not fully determined.

Here we describe a vastly improved FGE-based fluorophore labeling method. The protocol relies on efficient and controlled FGE conversion of Cys to fGly *in vitro* followed by specific and irreversible fluorophore labeling using the Hydrazinyl-Iso-Pictet-Spengler (HIPS) ligation method. Labeling requires ~150-fold less fluorophore and may be performed under mild solution conditions. We demonstrate efficient, site-selective, and large-scale preparation fluorophore-labeling of relatively labile EcMMR components that retained high specific activity. The portability of the FGE recognition sequence should make HIPS-fluorophore labeling widely applicable for single molecule imaging experiments as well as bulk and kinetic FRET interaction studies.

## Results

MMR is an excision-resynthesis reaction that repairs mismatched nucleotides that arise primarily as a result of polymerase misincorporation errors<sup>28</sup>. The initial recognition of mismatched nucleotide is carried out by MutS homologs (MSHs)<sup>29–31</sup>. MSH proteins form a long-lived mismatch-provoked ATP-bound sliding clamp that recruits MutL homologs (MLH/PMS)<sup>32</sup>; ultimately authorizing strand-specific excision and repair. The majority of single molecule MMR studies have used a singlet-Cys *Thermus aquaticus* TaMutS labeled with a maleimide-functionalized fluorophore<sup>19,21</sup>. Single molecule imaging of EcMutS and EcMutL (as well as other MSH and MLH/PMS proteins) is correspondingly difficult since they contain multiple structurally essential Cys residues.

Based on the prototypical FGE-based fluorophore labeling method described by Shi *et al.*<sup>1</sup>, we modified the largely disordered C-terminus of EcMutS to contain tandem hexa-histidine (his<sub>6</sub>) and FGE (LCTPSR; ald<sub>6</sub>) tags (EcMutS-his<sub>6</sub>/ald<sub>6</sub>; Table S1). The his<sub>6</sub> was separated from the EcMutS C-terminus by two Ser residues and the ald<sub>6</sub> was separated from the his<sub>6</sub> by two Gly residues. The EcMutS-his<sub>6</sub>/ald<sub>6</sub> was shown to genetically suppress the elevated mutation rates associated with *E. coli*  $\Delta$ mutS mutator phenotype ensuring that the tags did not interfere with *wild type* activities (Fig. S1). Two compatible plasmids were constructed to simultaneously express EcMutS (pET29a backbone) and *Mycobacterium tuberculosis* MtFGE (pBAD42 backbone)<sup>1</sup>. The EcMutS-his<sub>6</sub>/ald<sub>6</sub> was enriched using a Ni-NTA column, labeled with Cy3-hydrazide fluorophore<sup>1</sup> and free-dye removed using Heparin column chromatography. MonoQ chromatography resulted in >95% purified EcMutS-his<sub>6</sub>/ald<sub>6</sub>. We observed ~1% fluorophore-labeled protein in the presence of 4 mM Cy3-hydrazide (Fig. S2A), which increased to 5% fluorophore-labeled protein with 13 mM Cy3-hydrazide (Fig. S2B). When we increased the Cy3-hydrazide dye concentration to 66 mM, which was below the 75.6 mM dye concentration recommended by Shi *et al.*<sup>1</sup>, we observed ~30% fluorophore-labeled protein. However, virtually all of the EcMutS was insoluble under these conditions and became refractory to further purification (Fig. S3A). A similar precipitation propensity was observed when EcMutL-his<sub>6</sub>/ald<sub>6</sub>, EcRecJ-his<sub>6</sub>/Ald<sub>6</sub> and HsMSH2-ald<sub>6</sub>-HsMSH6-his<sub>6</sub> containing virtually identical his<sub>6</sub>/ald<sub>6</sub> tags labeled with Cy3- or Cy5-hydrazide (Fig. S3A; data not shown). We altered the central Cys residue to Ala in the ald<sub>6</sub>-tag [EcMutS-his<sub>6</sub>/ald<sub>6</sub>(C865A); Table S1] to examine the specificity of Cy3-hydrazide (66 mM) fluorophore labeling. We found that only 30% of the fluorophore-labeled EcMutS-his<sub>6</sub>/ald<sub>6</sub> protein could be considered specifically linked to the fGly residue (~9% of the total protein; Fig. S3B). These results suggested that the high concentrations of hydrazide-dyes induced solution instability of EcMutS and that hydrazide-fluorophore labeling of the ald<sub>6</sub>-tagged MMR protein was largely non-specific.

Previous observations have suggested that the labeling efficiency of hydrazide-functionalized fluorophores might be compromised by the low equilibrium constants associated with hydrazone formation in solution<sup>33</sup>. Moreover, the instability of the hydrazone bond results in shortened half-lives for hydrazone-labeled proteins<sup>34</sup>. In contrast, the Hydrazinyl-Iso-Pictet-Spengler (HIPS) ligation reaction has been shown to produce stable and irreversible covalent conjugates with reactive aldehydes at neutral pH<sup>35,36</sup>.

We conjugated a HIPS linker to cadaverine-modified Alexa-Fluor (AF) fluorophores (AF488, AF555, AF594 and AF647) as well as NHS-ester modified Atto488 similar to a previously described procedure (Fig. 1; Supplementary Materials and Methods)<sup>36</sup>. Partially purified Maltose Binding Protein containing an ald<sub>6</sub>-tag (MBP-ald<sub>6</sub>) was used as a fluorophore-labeling target. Mass spectroscopic (MS) analysis suggested that the ratio of fGly:Cys in the MBP-ald<sub>6</sub> preparation was 99:1, and that ~80% of these fGly residues could be linked to a HIPS-fluorophore<sup>26</sup>. However, MS may not detect FGE-converted Cys residues that have been subsequently altered or degraded to non-reactive chemical forms. We found that fluorophore conjugation to the MBP-ald<sub>6</sub> substrate induced a visible molecular weight shift in SDS-PAGE gels that allowed easy quantification of unlabeled (U) and specifically labeled (S) protein (Fig. 2A). Using this assay we determined that the absolute reactivity of the MBP-ald<sub>6</sub> substrate under identical solution conditions to our previous studies<sup>26</sup> was initially linear and saturated at 85% total labeling at 37 °C (Fig. 2A,

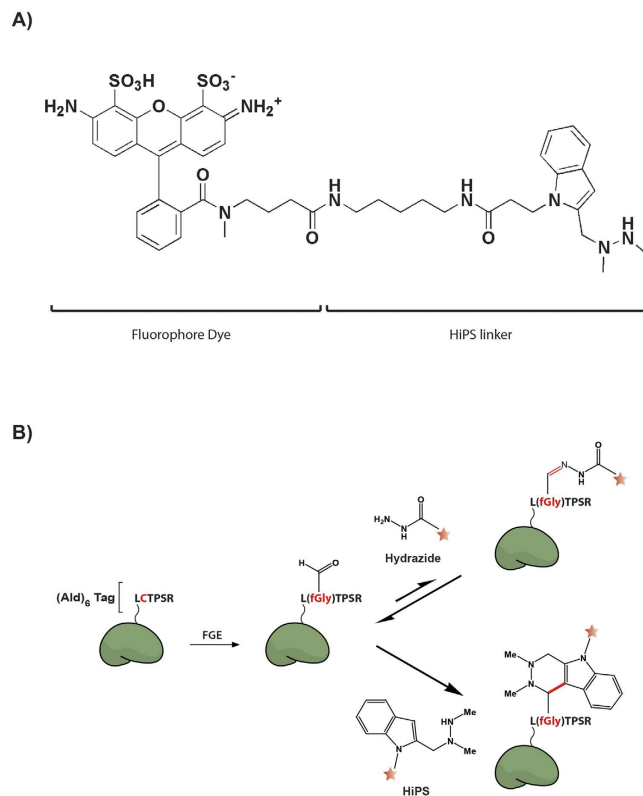


**Figure 1. HIPS-fluorophore chemical structure. (A)** Structure of the Atto488-Hydrazino-Pictet-Spengler (HIPS) fluorophore showing the Dye and HIPS linker. **(B)** The reaction scheme for the ald<sub>6</sub>-protein with the Hydrazide or HiPS-dyes.

red). We noted higher molecular weight bands (M) at fluorophore concentrations above 0.2 mM, suggesting non-specific fluorophore labeling as the specific fGly-fluorophore linking approached saturation.

Because of the comparative instability of MMR proteins we wished to examine fluorophore labeling at 0°C where these proteins may retain maximum activity over several days. At 0°C we found that MBP-ald<sub>6</sub> labeling saturated at 55% total labeling (Fig. 2A, black). The lower level of labeling saturation at 0°C compared to 37°C likely reflects different equilibrium dynamics. Saturation of fluorophore labeling at 0°C occurred between 2–5 mM HIPS-AF647 after 48 h (Fig. 2A, black) and at 96 h with 2 mM HIPS-AF647 (Fig. 2B). These HIPS-based fluorophore-labeling observations provided well-defined experimental windows to explore efficient labeling of MMR proteins.

The fGly conversion of the ald<sub>6</sub>-tag *in vivo* may vary between different protein substrates<sup>1,26,37</sup>. We found lower expression levels of MtFGE when co-expressed with EcMutS (Fig. S4A) as well as insolubility when MtFGE was expressed alone (Fig. S4B). These expression issues appeared to greatly attenuate the conversion reaction *in vivo*. Moreover, there are multiple other cellular enzymes that may catalyze the chemical modification of aldehydes *in vivo*<sup>38–40</sup> resulting in an obligate reduction in reactivity. As an alternative, we developed an FGE conversion step *in vitro* as an approach to control and retain fGly reactive aldehydes<sup>27,41</sup>. To examine the conversion efficiency with MMR proteins, EcMutS-his<sub>6</sub>/ald<sub>6</sub> was partially purified using Ni-NTA and incubated with partially purified his<sub>6</sub>-FGE at a ratio of 1:1 (7 μM ea) for varying times at 4°C (Fig. 3A,B). We observed a near linear relationship between the MtFGE incubation time and the relative labeling efficiency of EcMutS-his<sub>6</sub>/ald<sub>6</sub> with HIPS-Atto488 (2 mM) up to 48 h that was followed by reaction saturation. The use of a 1:1 ratio of MtFGE to target MMR protein appears to suggest that the conversion reaction is not catalytic. However, we performed the fGly conversion reaction at 4°C where turnover of the enzyme is known to be quite slow<sup>42</sup>. When conversion is performed at higher temperatures, the reaction becomes catalytic with ratios of target to FGE of 100–1000:1<sup>42</sup>. Interestingly, the labeling kinetics of EcMutS-his<sub>6</sub>/ald<sub>6</sub> with HIPS-AF555 (0.4 mM) was rapid and non-linear for the first 3 h to ~20% labeling followed by an apparently linear slower kinetics up to 72 h (Fig. S5A,B). However, subtraction of the 10% “nonspecific” labeling (see Fig. 4D) from each time-point results in a labeling curve (Fig. S5C), that appeared similar to the MBP-ald<sub>6</sub> labeling curve (Fig. 2B). We also noted fluorophore labeling of the MtFGE, which has been ascribed to auto-conversion<sup>43</sup>.

We examined the pH dependence of fGly conversion (Fig. 3C,D). While fluorophore-labeling appeared slightly greater at pH 9.1, we determined that the optimum pH for sufficient EcMutS-his<sub>6</sub>/ald<sub>6</sub> conversion that fully preserved the enzyme activity was pH 8.3. To examine the general applicability of our method

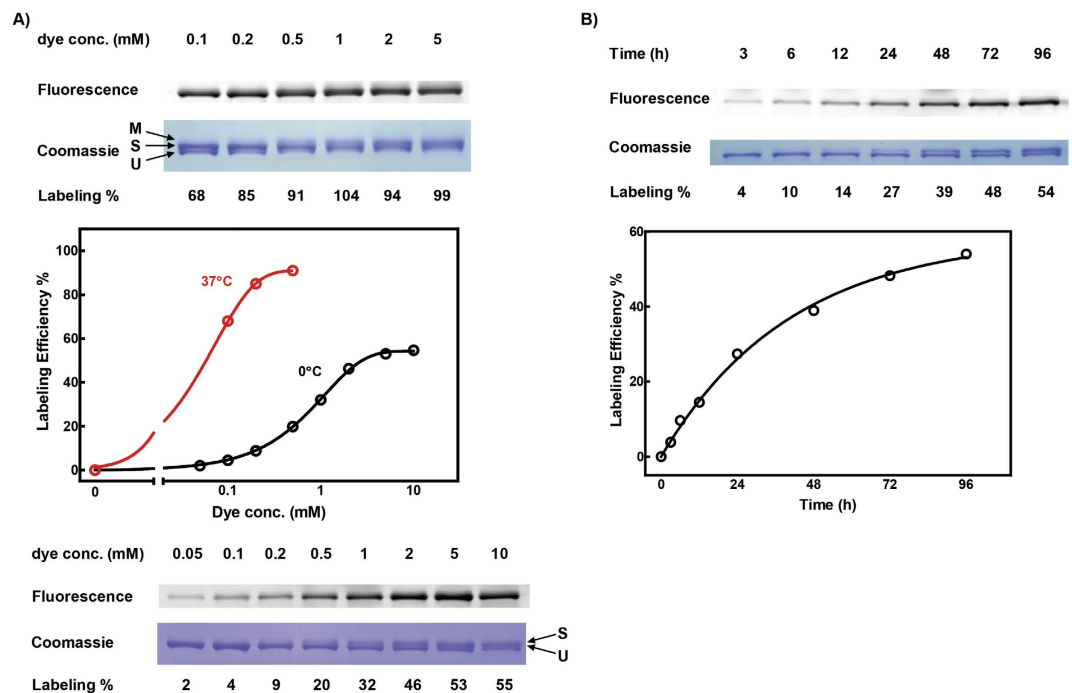


**Figure 2. HIPS-fluorophore labeling analysis.** Maltose Binding Protein (MBP) containing an FGE recognition sequence in which ~99% of the central cystein was converted to fGly (MBP-ald<sub>6</sub>) was used to determine labeling efficiency<sup>26</sup>. **(A)** (top panels) fluorophore dye concentration, the fluorescence scan of the PAGE gel and the coomassie stained PAGE gel of MBP-ald<sub>6</sub> following HIPS ligation at 37°C (graphed in middle panel). The coomassie stained PAGE gel shows the location of the unlabeled (U), single-labeled (S) and multiply labeled (M) HIPS-fluorophore. We noted that above 0.2 mM HIPS-dye at 37°C the quantity of protein that was labeled with more than one dye became significant reducing the quantification accuracy of specific labeling to the FGE-converted fGly. (bottom panels) the fluorophore dye concentration, the fluorescence scan of the PAGE gel and the coomassie stained PAGE gel of MBP-ald<sub>6</sub> following HIPS ligation at 0°C (graphed in middle panel). **(B)** Kinetics of HIPS-dye labeling to MBP-ald<sub>6</sub>. Top panels show time of incubation, the fluorescence scan of the PAGE gel and the coomassie stained PAGE gel of MBP-ald<sub>6</sub> following HIPS ligation at 0°C. Labeling efficiency was calculated as described in the Materials and Methods and accounts for loading variations between lanes. The Fluorescent scans and Coomassie stained gels have been cropped to show only the relevant protein bands, which in these studies accounts for >80% of the visible bands.

we introduced an ald<sub>6</sub>-tag onto the C-terminus of EcMutL (EcMutL-his<sub>6</sub>/ald<sub>6</sub>) and an internal site of EcMutL [EcMutL(346 ald<sub>6</sub>)-his<sub>6</sub>] that genetically complemented isogenic  $\Delta mutL$  (Fig. S1). In addition, we examined the labeling efficiency of the 5' → 3' MMR exonuclease EcRecJ (EcRecJ-his<sub>6</sub>/ald<sub>6</sub>). We found FGE-dependent conversion and labeling that was clearly specific compared to contaminating peptides in the partially purified MMR protein fractions (Fig. S6). Interestingly, we found that SDS-PAGE could separate labeled from unlabeled EcMutL monomer (Fig. S6C). Using simple Gaussian fits we determined that that 35% of the [EcMutL(346 ald<sub>6</sub>)-his<sub>6</sub>] appeared to be singly labeled with AF647.

The specificity of HIPS-fluorophore and Hydrazide-fluorophore labeling was quantitatively examined using the EcMutS-his<sub>6</sub>/ald<sub>6</sub>(C865A) substitution mutation (Fig. 4A; Fig. S7A). In the absence of FGE conversion *in vitro* we observed dramatically reduced fluorophore labeling of EcMutS-his<sub>6</sub>/ald<sub>6</sub>, which was further reduced at least 2-fold with the EcMutS-his<sub>6</sub>/ald<sub>6</sub>(C865A) substitution mutation (Fig. 4B; Fig. S7A). This labeling trend was consistent for three different HIPS-modified AF fluorophores (Fig. 4B; Fig. S7A). As a control we found that the labeling efficiency using hydrazide-modified AF555 was reduced an additional 2–3 fold compared to labeling with HIPS-modified AF fluorophores (Fig. 4B, yellow). Following FGE conversion *in vitro* the labeling efficiency of the HIPS-modified fluorophores increased 8–10 fold (Fig. 4B; Fig. S7A), while the labeling efficiency of the hydrazide-modified AF555 increased no more than 2-fold. We also demonstrate that the AF-HiPS dyes are stable and insensitive to SDS and boiling during sample preparation (compare Fig. S7A,B). These results are consistent with our previous conclusion that FGE conversion *in vitro* significantly enhances HIPS-modified fluorophore labeling efficiency. In addition, the hydrazide-modified fluorophores display substantially reduced labeling efficiency compared to HIPS-modified fluorophores.

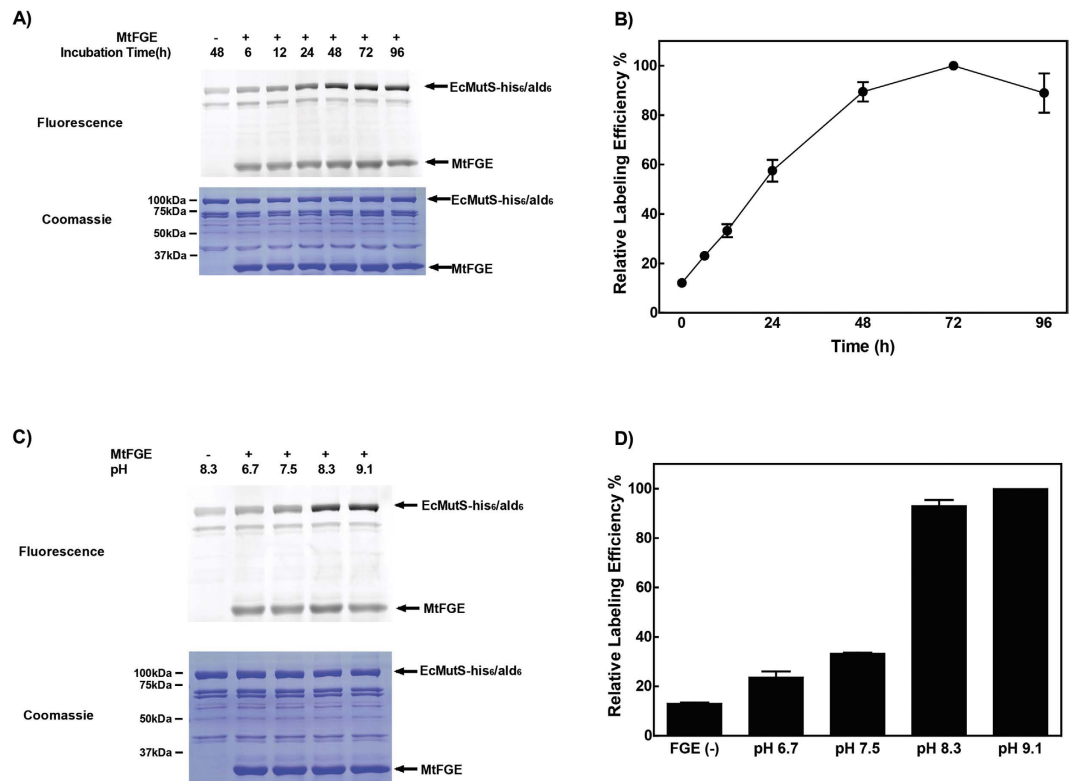


**Figure 3. FGE conversion *in vitro* enhances HIPS-fluorophore labeling.** (A) Fluorescent scan and coomassie stained gel of the FGE conversion *in vitro* kinetics using 2 mM HIPS-Atto488. (B) The fluorescent signal relative to the coomassie signal was quantified (Molecular Dynamics Image Quant), followed by setting the maximum ratio in the analysis to 100% to normalized the relative labeling efficiency of EcMutS-his<sub>6</sub>/ald<sub>6</sub> (see Material and Methods). (C) Fluorescent scan and coomassie stained gel of the pH-dependence of FGE conversion *in vitro* using 2 mM HIPS-Atto488. (D) The fluorescent signal relative to the coomassie signal was quantified (Molecular Dynamics Image Quant), followed by setting the maximum ratio in the analysis to 100% to normalized the relative labeling efficiency of EcMutS-his<sub>6</sub>/ald<sub>6</sub> (see Material and Methods).

In the absence of FGE conversion *in vitro*, <50% of the fluorophore label was specific for the fGly within the ald<sub>6</sub>-tag (Fig. 4C; Fig. S7). Moreover, the specificity of the hydrazide-modified AF555 in the absence of FGE conversion *in vitro* was near background. In the presence of FGE conversion *in vitro* the labeling efficiency was >90% specific for the fGly within the ald<sub>6</sub>-tag (Fig. 4D). In contrast, even with extreme excess of fluorophore the hydrazide-modified AF555 exhibited >5-fold less relative labeling in which at least 30% was not specific for the fGly within the ald<sub>6</sub>-tag (Fig. 4D; Fig. S7). Taken as a whole, these results suggest that combining FGE conversion of the ald<sub>6</sub>-tag *in vitro* followed by labeling with HIPS-modified fluorophores dramatically enhanced labeling efficiency and specificity.

We examined the stability of the HIPS-fluorophore conjugate to EcMutS-his<sub>6</sub>/ald<sub>6</sub> (Fig. S8A,B). Following incubation at 25 °C for 24 h we detected less than 0.7% loss of fluorophore (Fig. S8A,B). While the stability of a hydrazone-fluorophore conjugate could not be directly examined due to low labeling efficiency and solution instability, the stability of a related hydroxylamine-aldehyde conjugation that forms an aminoxy-aldehyde was determined (Fig. S8C). We found that 31% of the aminoxy-aldehyde fluorophore linkage was lost after 24 h at 37 °C (Fig. S8C). Moreover, 63% of the aminoxy-aldehyde conjugated fluorophore was lost after 6 d, while the HIPS-aldehyde lost only 16% after 6 d at 37 °C (Fig. S8C). It is important to note that the aminoxy-aldehyde conjugation has been reported to be to be far more stable than the hydrazide/hydrazone-aldehyde bond<sup>34</sup>, suggesting that HIPS-conjugated fluorophores are significantly more stable than hydrazide-conjugated fluorophores.

The lack of efficient and specific fluorophore labeling protocols has limited the rigorous examination of bulk and single molecule kinetic interactions between MMR proteins. Since EcMutS and EcMutL largely exist as stable dimers<sup>44,45</sup>, we calculated that 30% monomer labeling would result in 9% containing two fluorophores. Based on the MBP-ald<sub>6</sub> data (Fig. 2A,B), we performed FGE-HIPS fluorophore labeling using 0.5 mM HIPS-AF647 (4.8 mg) with 40 μM (30 mg) of EcMutS-his<sub>6</sub>/ald<sub>6</sub> and 0.5 mM HIPS-AF555 (0.6 mg) with 15 μM (1.5 mg) EcMutS-his<sub>6</sub>/ald<sub>6</sub>(D835R,R840E). The EcMutS(D835R,R840E) substitution mutations eliminate interaction between EcMutS dimers *in vitro* but do not appear to affect

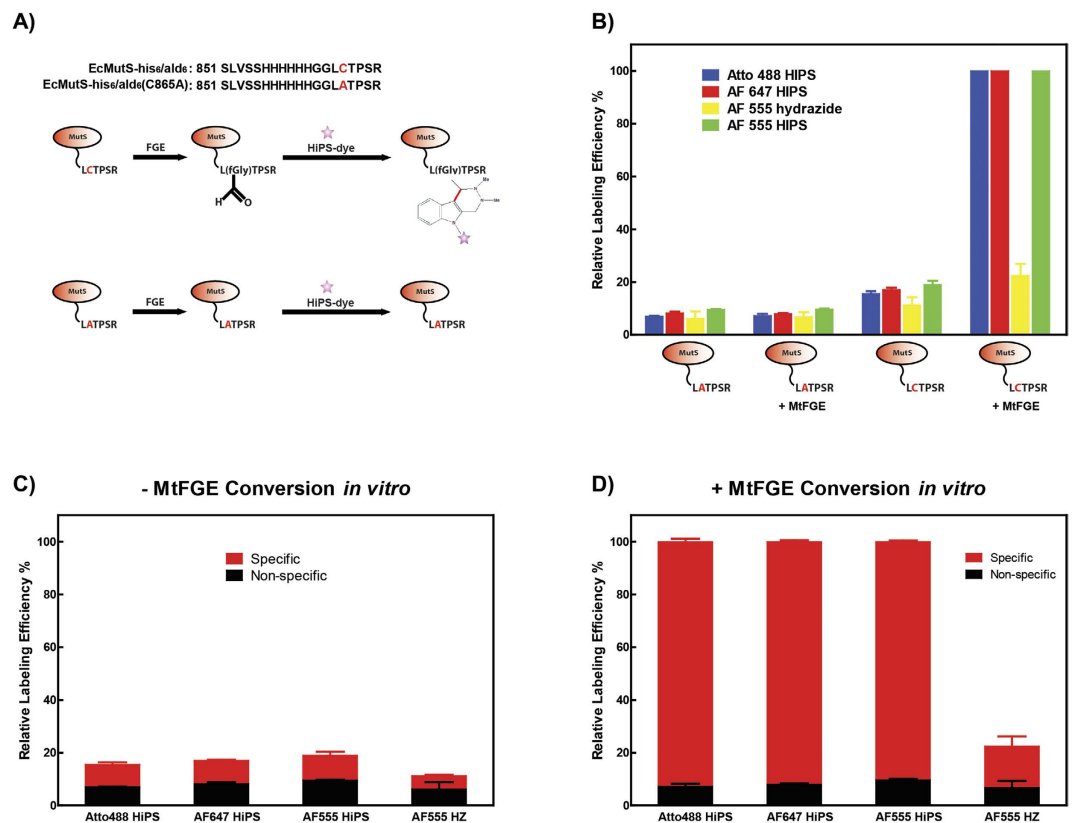


**Figure 4. HIPS-fluorophore ligation to fGly within an FGE site is highly specific.** (A) C-terminal sequences of EcMutS-his<sub>6</sub>/ald<sub>6</sub> and EcMutS-his<sub>6</sub>/ald<sub>6</sub>(C865A) as well as an illustration of HIPS-FGE labeling. (B) The normalized relative labeling efficiency (%) was calculated from Fig. S7 for EcMutS-his<sub>6</sub>/ald<sub>6</sub>(C865A) in the absence of MtFGE conversion *in vitro*, EcMutS-his<sub>6</sub>/ald<sub>6</sub>(C865A) following MtFGE conversion *in vitro* for 48 hrs, EcMutS-his<sub>6</sub>/ald<sub>6</sub> in the absence of MtFGE conversion *in vitro*, and EcMutS-his<sub>6</sub>/ald<sub>6</sub> following MtFGE conversion *in vitro* for 48 hrs each in the using the Atto488-HIPS (blue), AF647-HIPS (red), AF555-hydrazide (yellow), and AF555-HIPS fluorophore dyes (green). (C) The specificity of EcMutS-his<sub>6</sub>/ald<sub>6</sub> fluorophore-labeling in the absence of MtFGE conversion *in vitro*. Relative labeling efficiency (%) of EcMutS-his<sub>6</sub>/ald<sub>6</sub>(C865A) (black) is considered non-specific and the relative labeling efficiency (%) of EcMutS-his<sub>6</sub>/ald<sub>6</sub> minus the relative labeling efficiency (%) of EcMutS-his<sub>6</sub>/ald<sub>6</sub>(C865A) is considered specific for the FGE site (red). (D) The specificity of EcMutS-his<sub>6</sub>/ald<sub>6</sub> fluorophore-labeling in the presence of MtFGE conversion *in vitro* for 48 hrs. Specific and non-specific labeling were calculated as in panel (C).

MMR-dependent mutation suppression *in vivo*<sup>46</sup>. The unreacted fluorophore and FGE were removed by Heparin chromatography resulting in a >95% purified protein (Fig. 5A–D). The final labeling efficiency was determined to be 23% with the EcMutS-his<sub>6</sub>/ald<sub>6</sub> (16 μM) and 34% with the EcMutS-his<sub>6</sub>/ald<sub>6</sub>(D835R,R840E) (11 μM; Fig. 5A–D; Fig. S9A,B; Table S2). Since there does not appear to be an absolute correlation with the ratio of fluorophore to protein concentration for these two EcMutS constructs, we ascribe the modest differences in labeling efficiency to ald<sub>6</sub>-tag accessibility during conversion and/or labeling.

We labeled and purified EcMutL-his<sub>6</sub>/ald<sub>6</sub> following the same protocol we developed for EcMutS-his<sub>6</sub>/ald<sub>6</sub> with minor modifications (Fig. 5E–F; Materials and Methods). We obtained 35% AF647 fluorophore-labeled monomer EcMutL-his<sub>6</sub>/ald<sub>6</sub> (18 μM), which translates to a calculated 46% of singly labeled dimers with an additional 12% of the dimers containing two-fluorophores (Fig. S9C; Table S2). We determined that 41% of the EcMutL appeared to be singly labeled with AF647 by SDS-PAGE analysis (Fig. 5F), which appears similar to the spectrophotometry measure (Fig. S9C). While there may be modest differences in labeling efficiency between MMR proteins, preparations and ald<sub>6</sub>-tag location within a peptide, these results suggest that the labeling curves generated with the MBP-ald<sub>6</sub> can be generalized to most ald<sub>6</sub>-tagged proteins. Taken together our studies suggest that the method of FGE-HIPS fluorophore conjugation is predictable, efficient, specific, stable and generally low cost compared to other fluorophore-labeling schemes.

Previous studies suggested that one might separate unlabeled from fluorophore-labeled protein using hydrophobic interaction chromatography<sup>1</sup>. We examined several hydrophobic chromatography matrices including Butyl-S Sepharose, Butyl Sepharose, Phenyl Sepharose or TSKgel Phenyl-5PW. However, none

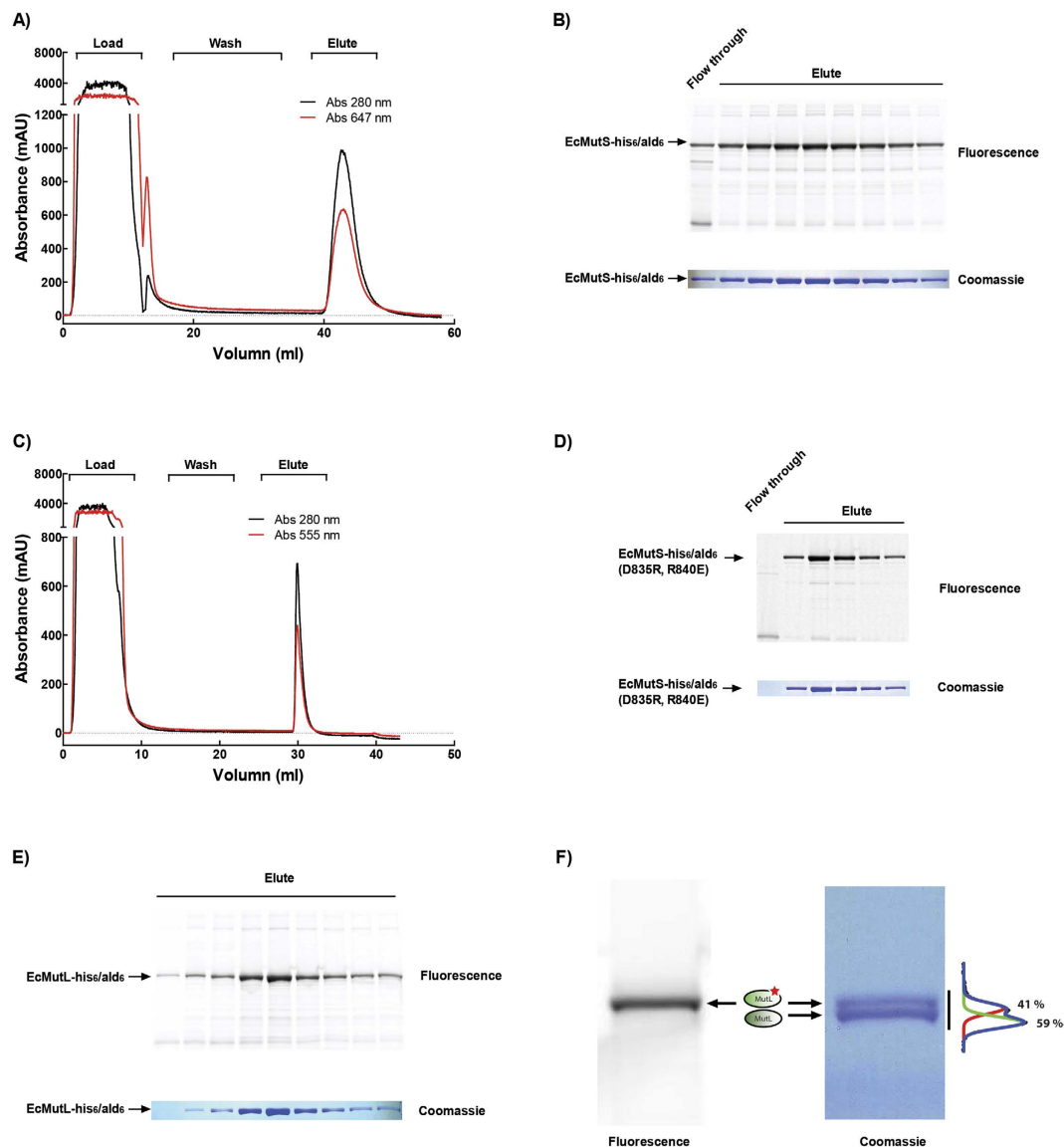


**Figure 5. HIPS fluorophore labeling and purification of EcMutS-his<sub>6</sub>/ald<sub>6</sub> and EcMutL-his<sub>6</sub>/ald<sub>6</sub>.**

(A,B) HIPS-AF647 fluorophore-labeling and purification of EcMutS-his<sub>6</sub>/ald<sub>6</sub>. Final heparin chromatography (A) and Fluorescence scan (top) and coomassie stain (bottom) of eluted fractions separated using SDS-PAGE gel (B). (C,D) HIPS-AF555 fluorophore-labeling and purification of EcMutS-his<sub>6</sub>/ald<sub>6</sub>(D835R,R840E). Final heparin chromatography (C) and Fluorescence scan (top) and coomassie stain (bottom) of eluted fractions separated using SDS-PAGE gel (D). (E,F) HIPS-AF647 fluorophore-labeling and purification of EcMutL-his<sub>6</sub>/ald<sub>6</sub>. Fluorescence scan (top) and coomassie stain (bottom) of eluted fractions separated using SDS-PAGE gel (E) and fluorescence scan (left) and coomassie stain (right) with Gaussian fitting of labeled (red) and unlabeled (green) EcMutL-his<sub>6</sub>/ald<sub>6</sub> (F). The Coomassie stained gels have been cropped to show only the relevant protein bands, which in these studies accounts for >90% of the visible bands.

of those approaches separated the highly specific fluorophore-labeled EcMutS from unlabeled protein (Fig. S10). We consider the possibility that hydrophobic chromatography utility may be linked to the solution exposure and/or hydrophobicity of the fluorophore<sup>1</sup>. Nevertheless, a labeling efficiency for proteins that approaches 50% is sufficient for most bulk FRET and single molecule studies.

We determined that the mismatch binding activity of EcMutS-his<sub>6</sub>/ald<sub>6</sub> during FGE-HIPS labeling and purification was similar and mismatch specific using electrophoretic mobility shift analysis (EMSA; Fig. S11). Real-time bulk kinetic analysis using Surface Plasmon Resonance (SPR; Biacore) revealed minor variations in  $k_{on}$ ,  $k_{off}$  and  $K_D$  between fluorophore-labeled and unlabeled EcMutS-his<sub>6</sub>/ald<sub>6</sub> or EcMutS-his<sub>6</sub>/ald<sub>6</sub>(D835R,R840E) that were within the standard error of the system (Table 1; Fig. S12). We also examined the ability of EcMutS-his<sub>6</sub>/ald<sub>6</sub> to form an ATP-bound sliding clamp by determining the  $k_{off,ATP}$  kinetics (Table 1). In all cases the rate appeared similar with the exception of the AF647-labeled

Protein	$k_{on}$ ( $10^5 \times M^{-1} \times sec^{-1}$ )	$k_{off}$ ( $10^{-4} \times sec^{-1}$ )	$K_D$ (nM)	$k_{off-ATP}$ ( $sec^{-1}$ )
AF555 labeled EcMutS- his <sub>6</sub> /ald <sub>6</sub> (D835R, R840E)	4.37 ± 0.90	24.48 ± 1.44	5.75 ± 1.51	0.45 ± 0.09
Unlabeled EcMutS- his <sub>6</sub> /ald <sub>6</sub> (D835R, R840E)	9.48 ± 3.90	33.02 ± 1.87	3.85 ± 1.78	0.48 ± 0.09
AF647 labeled EcMutS- his <sub>6</sub> /ald <sub>6</sub>	3.44 ± 0.52	8.93 ± 0.34	2.63 ± 0.49	0.26 ± 0.08
Unlabeled EcMutS- his <sub>6</sub> /ald <sub>6</sub>	5.29 ± 1.82	6.10 ± 0.53	1.25 ± 0.53	0.53 ± 0.11

**Table 1. DNA Binding, Dissociation and ATP Processing Constants for *E. coli* MutS.**

EcMutS-his<sub>6</sub>/ald<sub>6</sub>, which appeared to form a sliding clamp approximately 2-fold better than the unlabeled EcMutS-his<sub>6</sub>/ald<sub>6</sub>. All the kinetic rate constants of EcMutS-his<sub>6</sub>/ald<sub>6</sub> binding and dissociation reported here are similar to the values obtained for EcMutS (without ald<sub>6</sub>-tag) in previous studies<sup>32,47</sup>.

To demonstrate utility for *in singulo studies*, prism-based total internal reflection fluorescence (TIRF) microscopy was used to image single molecules of AF647-labeled EcMutS-his<sub>6</sub>/ald<sub>6</sub> and AF555-labeled EcMutS-his<sub>6</sub>/ald<sub>6</sub>(D835R,R840E) on a 17 Kb λ DNA containing a single mismatch (Fig. S13A,B). We observed many stable ATP-bound EcMutS sliding clamps that freely diffused along the entire length of the DNA (Fig. S13A,B)<sup>19,48</sup>. The 1-dimensional (1D) random walk particle diffusion characteristic was clearly visible and a diffusion coefficient for AF555-labeled EcMutS-his<sub>6</sub>/ald<sub>6</sub>(D835R,R840E) ( $D = 0.044 \mu m^2/sec \pm 0.014 \mu m^2/sec$ ,  $N = 77$ ) was easily calculated (Fig. S13A,B; Suppl. Movie-1 and Movie-2, respectively). While these are the first images of ATP-bound EcMutS sliding clamp diffusion on mismatched DNA, the observations appear similar to previous single molecule analysis of TaMutS and *Saccharomyces cerevisiae* ScMsh2-ScMsh6<sup>19,20,48</sup>. These studies demonstrate that HIPS fluorophore-labeled EcMutS is fully functional for multiple known MSH protein activities. Taken as a whole, our studies demonstrate the general applicability of the HIPS fluorophore-labeling method in bulk and single molecule fluorescence-based analysis.

## Discussion

Although some proteins tagged with an FGE recognition sequence contain converted fGly following co-expression of the FGE protein *in vivo*, this appears not to be the case for all proteins and definitely not with the *E. coli* MMR proteins. While the factors that allow significant conversion *in vivo* are not entirely clear, it appears that the ratio and distribution of soluble FGE and ald<sub>6</sub>-tagged protein are substantial contributors to conversion efficiency. Our results indicate that high expression of FGE may reduce the expression of an ald<sub>6</sub>-tagged protein in *E. coli*, while low expression of FGE can lead to incomplete fGly conversion and reduced labeling efficiency. Moreover, many cellular enzymes exist that may catalyze the modification of aldehydes *in vivo* rendering them unreactive<sup>38–40</sup>. We have found that the conversion of an ald<sub>6</sub>-tag to fGly *in vitro* is easily managed and may be used with partially purified proteins under conditions where unwanted post-conversion aldehyde products may be significantly reduced.

The development of a His<sub>6</sub>-tagged FGE that is easily overexpressed in *E. coli* and may be enriched in a single Ni-NTA chromatography step to >90% purity makes conversion *in vitro* extremely attractive. In addition we have constructed a His<sub>6</sub>-tagged FGE containing a human *Rinovirus* (HRV) 3C protease site capable of removing the his<sub>6</sub>-tag at 0°C. This latter construct allows conversion *in vitro* and HIPS fluorophore labeling in the presence of HRV 3C protease that may then be followed by Ni-NTA chromatography, which will remove both unincorporated HIPS-fluorophore and the FGE catalytic protein.

The dramatically reduced concentrations of HIPS modified fluorophores required for protein labeling makes this method significantly more cost effective than previous approaches<sup>26</sup>. In fact, the FGE-conversion *in vitro* and HIPS-fluorophore labeling (FGE-HIPS) system appears comparable in efficiency to maleimide-based Cys residue chemical labeling that we have previously used with TaMutS<sup>19</sup>. With the advent of commercially available HIPS-fluorophores, this technology should be widely useful to the scientific community. A major limitation to increasing labeling efficiency is the requirement that the MMR proteins must be maintained at 0°C in order to preserve specific activity. However, for proteins that maintain activity at elevated temperatures labeling efficiency may be dramatically increased such that at 20–37°C saturated labeling may occur in a matter of hours (Fig. 2A). In general, we find that labeling efficiency may be increased with higher concentration of fluorophore, longer labeling times, and elevated temperature. We also note that only site-specific labeling increases with longer labeling times (Fig. S5). However, in spite of 99:1 fGly:Cys conversion ratio the site-specific HIPS labeling reaction saturates at ~80%. It should be noted that this saturation efficiency is comparable to virtually all the current fluorophore labeling technologies and likely reflects labeling equilibrium dynamics. In conclusion, we have described an FGE-based fluorophore-labeling method that uses an fGly conversion step *in vitro* followed by Hydrazinyl-Iso-Pictet-Spengler ligation under mild solution conditions. The method displays high specificity with little, if any, effect on protein activity. The specificity of the FGE recognition sequence and relatively low cost of this method makes it generally useful for bulk and single molecule imaging studies that rely on fluorophore-labeling of component proteins.



## Methods

MMR genes were amplified by PCR with primers containing ald<sub>6</sub> (LCTPSR) tags and inserted into expression plasmids. Proteins were then purified from *E. coli* strains with the plasmids. Detail information are described in the Supplementary material.

MMR proteins containing an ald<sub>6</sub>-tag were converted with MtFGE *in vitro* and then changed into labeling buffer. HiPS dyes were then added to label the proteins. Detail information are described in the Supplementary material.

SPR experiments were performed as previously described<sup>49</sup> and the detail information are described in the Supplementary material.

A single molecule Fluorophore Tracking (smFT) apparatus constructed with prism-type Total Internal Reflection Fluorescence (TIRF) microscopy as described<sup>48</sup>. A 17 kb DNA with a single mismatch located 6 Kb from one end was constructed similar to our previous publication<sup>48</sup>. Detail information are described in the Supplementary material.

## References

- Shi, X. *et al.* Quantitative fluorescence labeling of aldehyde-tagged proteins for single-molecule imaging. *Nat Methods* **9**, 499–503 (2012).
- Selvin, P. R. & Ha, T. *Single Molecule Techniques: a laboratory manual*, (CSHL Press, Cold Spring Harbor, N.Y. 2008).
- Abbondanzieri, E. A. *et al.* Dynamic binding orientations direct activity of HIV reverse transcriptase. *Nature* **453**, 184–9 (2008).
- Liu, S., Abbondanzieri, E. A., Rausch, J. W., Le Grice, S. F. & Zhuang, X. Slide into action: dynamic shuttling of HIV reverse transcriptase on nucleic acid substrates. *Science* **322**, 1092–7 (2008).
- Lee, W., Jose, D., Phelps, C., Marcus, A. H. & von Hippel, P. H. A Single-Molecule View of the Assembly Pathway, Subunit Stoichiometry, and Unwinding Activity of the Bacteriophage T4 Primosome (helicase-primase) Complex. *Biochemistry* **52**, 3157–70 (2013).
- Ibarra, B. *et al.* Proofreading dynamics of a processive DNA polymerase. *EMBO J* **28**, 2794–802 (2009).
- Manosas, M., Perumal, S. K., Croquette, V. & Benkovic, S. J. Direct observation of stalled fork restart via fork regression in the T4 replication system. *Science* **338**, 1217–20 (2012).
- Mukhopadhyay, J. *et al.* Fluorescence resonance energy transfer (FRET) in analysis of transcription-complex structure and function. *Methods Enzymol* **371**, 144–59 (2003).
- Coban, O., Lamb, D. C., Zaychikov, E., Heumann, H. & Nienhaus, G. U. Conformational heterogeneity in RNA polymerase observed by single-pair FRET microscopy. *Biophys J* **90**, 4605–17 (2006).
- Kapanidis, A. N. *et al.* Initial transcription by RNA polymerase proceeds through a DNA-scrunching mechanism. *Science* **314**, 1144–7 (2006).
- Chakraborty, A. *et al.* Opening and closing of the bacterial RNA polymerase clamp. *Science* **337**, 591–5 (2012).
- Davenport, R. J., Wuite, G. J., Landick, R. & Bustamante, C. Single-molecule study of transcriptional pausing and arrest by *E. coli* RNA polymerase. *Science* **287**, 2497–500 (2000).
- Sakata-Sogawa, K. & Shimamoto, N. RNA polymerase can track a DNA groove during promoter search. *Proc Natl Acad Sci USA* **101**, 14731–5 (2004).
- Harada, Y. *et al.* Direct observation of DNA rotation during transcription by *Escherichia coli* RNA polymerase. *Nature* **409**, 113–5 (2001).
- Blanchard, S. C., Gonzalez, R. L., Kim, H. D., Chu, S. & Puglisi, J. D. tRNA selection and kinetic proofreading in translation. *Nat Struct Mol Biol* **11**, 1008–14 (2004).
- Uemura, S. *et al.* Real-time tRNA transit on single translating ribosomes at codon resolution. *Nature* **464**, 1012–7 (2010).
- Qu, X. *et al.* The ribosome uses two active mechanisms to unwind messenger RNA during translation. *Nature* **475**, 118–21 (2011).
- Blainey, P. C., van Oijen, A. M., Banerjee, A., Verdine, G. L. & Xie, X. S. A base-excision DNA-repair protein finds intrahelical lesion bases by fast sliding in contact with DNA. *Proc Natl Acad Sci USA* **103**, 5752–7 (2006).
- Jeong, C. *et al.* MutS switches between two fundamentally distinct clamps during mismatch repair. *Nat Struct Mol Biol* **18**, 379–85 (2011).
- Gorman, J. *et al.* Single-molecule imaging reveals target-search mechanisms during DNA mismatch repair. *Proc Natl Acad Sci USA* **109**, E3074–83 (2012).
- Qiu, R. *et al.* Large conformational changes in MutS during DNA scanning, mismatch recognition and repair signalling. *Embo J* **31**, 2528–40 (2012).
- Howan, K. *et al.* Initiation of transcription-coupled repair characterized at single-molecule resolution. *Nature* **490**, 431–4 (2012).
- Resch-Genger, U., Grabolle, M., Cavaliere-Jaricot, S., Nitschke, R. & Nann, T. Quantum dots versus organic dyes as fluorescent labels. *Nat Methods* **5**, 763–75 (2008).
- Hanne, J., Liu, J., Lee, J.-B. & Fishel, R. Single-molecule FRET Studies on DNA Mismatch Repair. *International Journal of Biophysics* **3**, 18–38 (2013).
- Roeser, D. *et al.* A general binding mechanism for all human sulfatases by the formylglycine-generating enzyme. *Proc Natl Acad Sci USA* **103**, 81–6 (2006).
- Carrico, I. S., Carlson, B. L. & Bertozzi, C. R. Introducing genetically encoded aldehydes into proteins. *Nat Chem Biol* **3**, 321–2 (2007).
- Rush, J. S. & Bertozzi, C. R. New aldehyde tag sequences identified by screening formylglycine generating enzymes *in vitro* and *in vivo*. *J Am Chem Soc* **130**, 12240–1 (2008).
- Friedberg, E. C. *et al.* *DNA Repair and Mutagenesis*, (American Society of Microbiology, Washington, D.C., 2006).
- Fishel, R. & Wilson, T. MutS homologs in mammalian cells. [Review] [84 refs]. *Curr Opin Genet Dev* **7**, 105–13 (1997).
- Kolodner, R. Biochemistry and genetics of eukaryotic mismatch repair. [Review] [85 refs]. *Genes & Development* **10**, 1433–42 (1996).
- Kolodner, R. D., Mendillo, M. L. & Putnam, C. D. Coupling distant sites in DNA during DNA mismatch repair. *Proc Natl Acad Sci USA* **104**, 12953–4 (2007).
- Acharya, S., Foster, P. L., Brooks, P. & Fishel, R. The coordinated functions of the *E. coli* MutS and MutL proteins in mismatch repair. *Molecular Cell* **12**, 233–46 (2003).
- Dirksen, A. & Dawson, P. E. Rapid oxime and hydrazone ligations with aromatic aldehydes for biomolecular labeling. *Bioconjug Chem* **19**, 2543–8 (2008).
- Kalia, J. & Raines, R. T. Hydrolytic stability of hydrazones and oximes. *Angew Chem Int Ed Engl* **47**, 7523–6 (2008).

35. Agarwal, P. *et al.* Hydrazino-Pictet-Spengler ligation as a biocompatible method for the generation of stable protein conjugates. *Bioconjug Chem* **24**, 846–51 (2013).
36. Agarwal, P., van der Weijden, J., Sletten, E. M., Rabuka, D. & Bertozzi, C. R. A Pictet-Spengler ligation for protein chemical modification. *Proc Natl Acad Sci USA* **110**, 46–51 (2013).
37. Wu, P. *et al.* Site-specific chemical modification of recombinant proteins produced in mammalian cells by using the genetically encoded aldehyde tag. *Proc Natl Acad Sci USA* **106**, 3000–5 (2009).
38. Vasiliou, V., Pappa, A. & Petersen, D. R. Role of aldehyde dehydrogenases in endogenous and xenobiotic metabolism. *Chem Biol Interact* **129**, 1–19 (2000).
39. Sophos, N. A. & Vasiliou, V. Aldehyde dehydrogenase gene superfamily: the 2002 update. *Chem Biol Interact* **143–144**, 5–22 (2003).
40. Ho, K. K. & Weiner, H. Isolation and characterization of an aldehyde dehydrogenase encoded by the aldB gene of *Escherichia coli*. *J Bacteriol* **187**, 1067–73 (2005).
41. Carlson, B. L. *et al.* Function and structure of a prokaryotic formylglycine-generating enzyme. *J Biol Chem* **283**, 20117–25 (2008).
42. Holder, P. G. *et al.* Reconstitution of Formylglycine-generating Enzyme with Copper(II) for Aldehyde Tag Conversion. *J Biol Chem* **290**, 15730–45 (2015).
43. Bojarova, P. & Williams, S. J. Sulfotransferases, sulfatases and formylglycine-generating enzymes: a sulfation fascination. *Curr Opin Chem Biol* **12**, 573–81 (2008).
44. Grilley, M., Welsh, K. M., Su, S. S. & Modrich, P. Isolation and characterization of the *Escherichia coli* mutL gene product. *J Biol Chem* **264**, 1000–4 (1989).
45. Su, S.-S. & Modrich, P. *Escherichia coli* mutS-encoded protein binds to mismatched DNA base pairs. *Proc. Natl. Acad. Sci. USA* **83**, 5057–5061 (1986).
46. Mendillo, M. L., Putnam, C. D. & Kolodner, R. D. *Escherichia coli* MutS tetramerization domain structure reveals that stable dimers but not tetramers are essential for DNA mismatch repair *in vivo*. *J Biol Chem* **282**, 16345–54 (2007).
47. Martin-Lopez, J. *et al.* The hMSH2(M688R) Lynch Syndrome Mutation may Function as a Dominant Negative. *Carcinogenesis* **33**, 1647–1654 (2012).
48. Cho, W. K. *et al.* ATP Alters the Diffusion Mechanics of MutS on Mismatched DNA. *Structure* **20**, 1264–74 (2012).
49. Mazurek, A., Johnson, C. N., Germann, M. W. & Fishel, R. Sequence context effect for hMSH2-hMSH6 mismatch-dependent activation. *Proc Natl Acad Sci USA* **106**, 4177–82 (2009).

## Acknowledgements

The authors would like to thank members of the Fishel lab for helpful discussions. This work was supported by NIH grants CA67007 and GM080176 (R.F.).

## Author Contributions

J.L., D.R., J.-B.L. and R.F. designed the studies; J.L. J.H., B.M.B performed the studies; M.S. contributed to data analysis; A.A., J.B., R.Z. and R.B. contributed data and reagents; J.L. and R.F. wrote the manuscript.

## Additional Information

**Supplementary information** accompanies this paper at <http://www.nature.com/srep>

**Competing financial interests:** Several authors are associated with Catalent Biologics that hold patents to the HiPS linker technology. Calalent Biologics reserves the right to commercialize and/or license HiPS-fluorophore production, that are the fundamental labeling reagents described in this manuscript.

**How to cite this article:** Liu, J. *et al.* An Efficient Site-Specific Method for Irreversible Covalent Labeling of Proteins with a Fluorophore. *Sci. Rep.* **5**, 16883; doi: 10.1038/srep16883 (2015).



This work is licensed under a Creative Commons Attribution 4.0 International License. The images or other third party material in this article are included in the article's Creative Commons license, unless indicated otherwise in the credit line; if the material is not included under the Creative Commons license, users will need to obtain permission from the license holder to reproduce the material. To view a copy of this license, visit <http://creativecommons.org/licenses/by/4.0/>